Materials and Design 30 (2009) 459–468

Contents lists available at ScienceDirect

Materials and Design

journal homepage: www.elsevier.com/locate/matdes

Experimental investigation of explosive welding of cp-titanium/AISI 304 stainless steel

S.A.A. Akbari Mousavi *, P. Farhadi Sartangi

School of Metallurgy and Materials Engineering, University College of Engineering, University of Tehran, P.O. Box 11365-4563, Tehran, Iran

ARTICLE INFO

Article history:
Received 13 March 2008
Accepted 2 June 2008
Available online 13 June 2008

Keywords:
Welding (D)
Fracture (E)
Metallography (G)

ABSTRACT

In explosive welding process, the controlled energy of explosives is used to create a metallurgical bond between two similar or dissimilar materials. This paper presents the analytical calculation for determination of weldability domain or welding window. The analytical calculations are in good agreement with experimental results. The welding conditions are tailored through parallel geometry route with different explosive loads. The study was also conducted to consider the effects of explosive loading on the bonding interface and the characterization of explosive welding experiments carried out under different conditions. Optical microscopy studies show that a transition from a smooth interface to a wavy one occurs with increase in explosive load. Scanning electron microscopy studies show that the interface was outlined by characteristic sharp transition between two materials, but local melted zones were also encountered in the front slope of waves in the interface at high explosive loads. XRD studies detected no intermetallic phases for specimen welded at low explosive load.

1. Introduction

Explosive welding offers an excellent alternative for joining dissimilar metals and alloys with varying physical and metallurgical properties. Explosive welding is a solid state metal joining process which produces a weld joint by high velocity oblique impact, aided by controlled detonation with an explosive charge [1,2]. The explosive charge when detonated accelerates the plates to a speed at which a metallic bond is formed between the metal components during the collision. The metal plates are made to collide obliquely with each other at high velocity with the use of explosive. During the high velocity oblique collision of metal plates, a high velocity jet is formed between the metal plates if the impact angle β and impact velocity, V_p, are in the range required for bonding (Fig. 1) [1,2]. The oxide films are detrimental to the establishment of the metallurgical bond. These films are swept away from the interface by the jet. The metal plates are then cleaned of any surface film by the jet action. At the collision point, virginally clean surface are brought together under very high pressure [1]. The pressure has to be sufficiently high and for a sufficient length of time to achieve inter-atomic bonds. The velocity of the collision point, V_c, governs the time available for bonding. This high pressure also causes considerable local plastic deformation of the metals in the bond zone [1,3,4]. The bond is metallurgical in nature and usually is stronger than the weaker material [1,2]. Some authors considered the explosive bonding as a cold pressure welding without thermally activated process [5]. However, in the explosive welding, a molten layer is found in the interface for clads fabricated with inappropriate parameters such as excess charge of explosive [2]. On the other hand, a few reports based on TEM observations suggested that thermally activated processes take place within the bonding zone and bonding is achieved by melting of thin layers along the contact surface of the two plates [6].

The quality of the bonds strongly depends on careful control of the process parameters. These include material surface preparation, plate separation or stand-off distance, explosive load or explosive ratio, detonation energy and detonation velocity, V_d. The selection of parameters is based upon the mechanical properties, density and shear wave velocity of each component [1–5]. Considerable progress has been made to establish the optimum operational parameters which are required to produce an acceptable bond. For this reason welding windows of various parameters such as collision velocity-impact angle or flyer plate velocity-impact angle were proposed by different authors [7–10].

The selection of an explosive that will produce the required detonation velocity is the most important factor for obtaining consistent good welds. It has been shown that the collision velocity V_c and the plate velocity V_p should be less than the velocity of sound in either welding component [11–14]. The velocity of sound in engineering materials is typically 4.5–6 km/s, whereas the detonation velocity in common explosive (plastic explosive) is typically 6–7 km/s. The high velocity explosives are not suitable

* Corresponding author. Tel.: +98 21 82084096; fax: +98 21 88006076.
E-mail addresses: akbarimusavi@ut.ac.ir (S.A.A. Akbari Mousavi), farhadi_pezhman@engmail.ut.ac.ir (P. Farhadi Sartangi).

0261-3069/$ - see front matter © 2008 Elsevier Ltd. All rights reserved.
doi:10.1016/j.matdes.2008.06.016

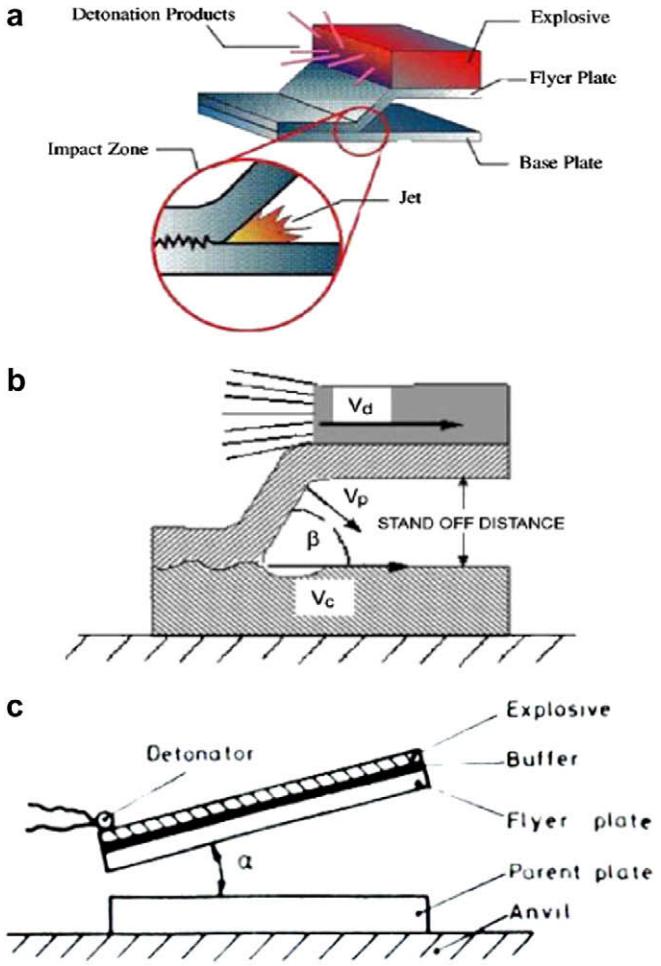

Fig. 1. (a) Explosive welding process, (b) explosive welding parameters – parallel geometry and (c) explosive welding process – inclined geometry.

for explosive welding [1,7–14]. A mixture of ammonium nitrate and fuel oil (ANFO) and an inert substance such as sand or perlite is often used with detonation velocity typically between 2 and 3 km/s for this purpose [1,5,11]. The explosive must also provide uniform detonation so as to achieve a collision velocity that will be uniform from the start to finish of the weld. The explosive type and amount per unit area is selected to achieve the necessary detonation energy and detonation velocity [1–5].

Wavy interface is the characteristic feature of explosive welds. The wave formation in explosive welding can be regarded as a special case of general phenomena of interfacial wave formation under certain flow circumstance. Wave formation appears to be the result of variations in the velocity distribution at collision point and periodic disturbances of materials [1,3,4].

Cladding of flat plates and concentric cylinders constitutes the major commercial application of explosive welding [1,5]. Advantageous features of explosive cladding include: the joining of dissimilar metals together; the bonding of thin sheet with thick plates; the welding of heat-treated and cold worked metals together without change in their mechanical properties; the absence of heat affected zone in the clad plates and the simplicity and speed of operation for having coalescence with cost reduction and strength or corrosion properties [1,5–14].

Titanium's superior corrosion resistance is ideal for many process applications. Process industries choose titanium as the material of construction for piping, tanks, pressure vessel, autoclaves and heat exchangers. When pressure and/or temperatures and size

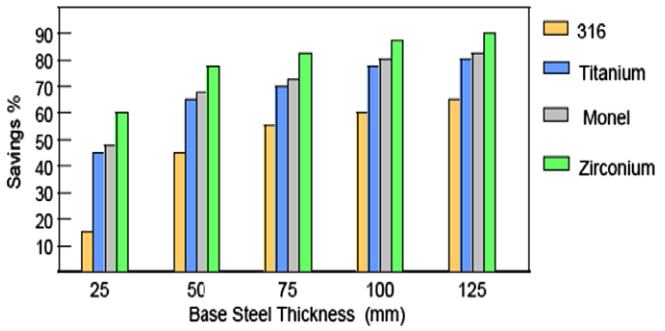

Fig. 2. Typical cost savings of explosion clad compared to solid alloy of equal thickness (3 mm thick alloy clad onto steel).

demand very thick plates, the titanium equipment can become considerably more expensive than units constructed from lower cost, lower performance materials. Titanium clad steel provides lower cost than many other materials as indicated in Fig. 2. The explosion cladding process produces a high quality titanium–steel clad product with proven fabrication reliability and performance [15–20].

It is known that the quality and morphology of the interface depend on the collision angle, the impact velocity, and the properties of the materials and the geometry of the welded plates [1,3,11].

The objective of this study, whose results are described herein, was to determine the operational parameters for cladding of titanium to stainless steel plates. In the first part of the study, the welding window of Ti/stainless steel is developed by using the equations suggested by various researchers. The welding window enables the establishments of analytical conditions for the formations of wavy and smooth bond interfaces. The second part of the study discusses the various interface morphology obtained from experiments. In this study, all the experiments are carried out in parallel arrangements (see Fig. 1b), in which the welding velocity is equal to the detonation velocity. The experiments were carried out with various explosive loads and constant stand-off distance. The collision angle β is obtained from the collision and plate velocities by simple geometrical considerations. The study was conducted to consider the effects of explosive loading on the microstructure of the interface morphology using the optical and scanning electron microscope. Furthermore, various types of intermetallic phases produced at the interface under various explosive loading are examined by the X-ray diffraction analysis.

2. Analyses

2.1. The smooth–wavy transition criteria

A model capable of predicting the wave geometry would be able to determine the smooth–wavy transition. This enables us to adopt experimental conditions for the formation of the wavy and smooth interfaces. The hydrodynamic analogy has been frequently used for the prediction of the wave properties which describes wave formation as being analogous to fluid flow behind an obstacle, i.e. the smooth–wavy boundary corresponds to the laminar-turbulent transition. In fluid mechanics, Reynolds number characterizes this transition. Cowan et al. [21–23] introduced the following Reynolds number R_t for explosive welding:

$$R_t = (\rho_a + \rho_b)V_f^2/2(H_a + H_b) \quad (1)$$

where ρ_a and ρ_b are the densities of the materials and H_a and H_b are their Vickers hardnesses. V_f is the velocity of the flyer plate relative to an observer moving with stagnation point S (see Fig. 3). V_{ct} in Fig. 4 resembles V_f in Fig. 3.

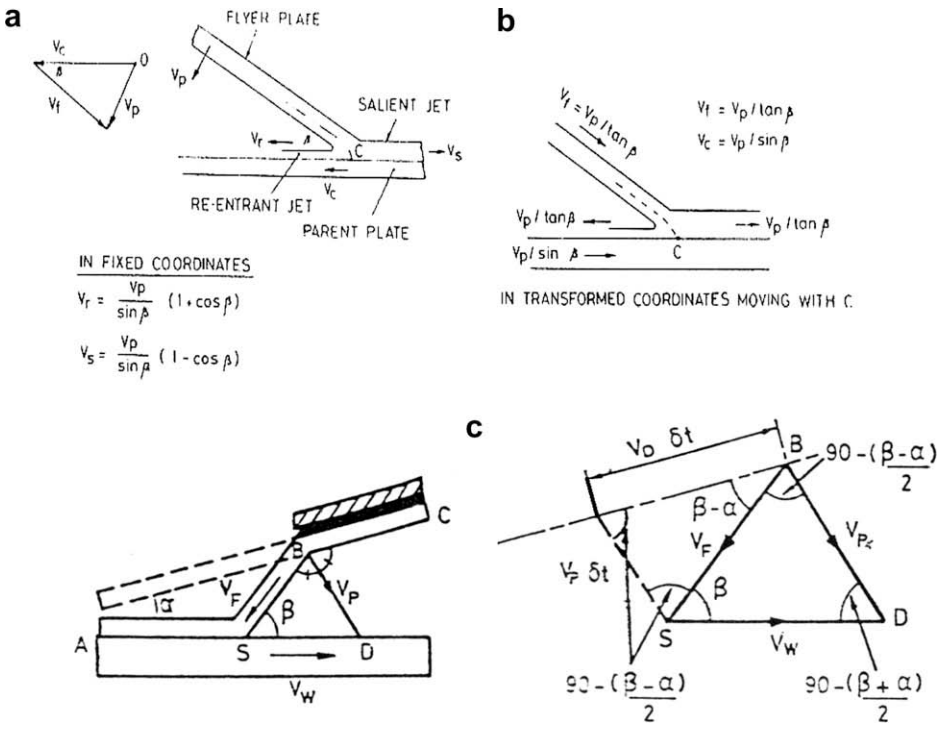

Fig. 3. (a) Geometry of collapse of flyer plate in fixed coordinates (parallel geometry), (b) geometry of collapse of flyer plate in transformed coordinates moving with C (parallel geometry) and (c) geometry of collapse of flyer plate (Inclined geometry), (Birkholf et. al. [12]).

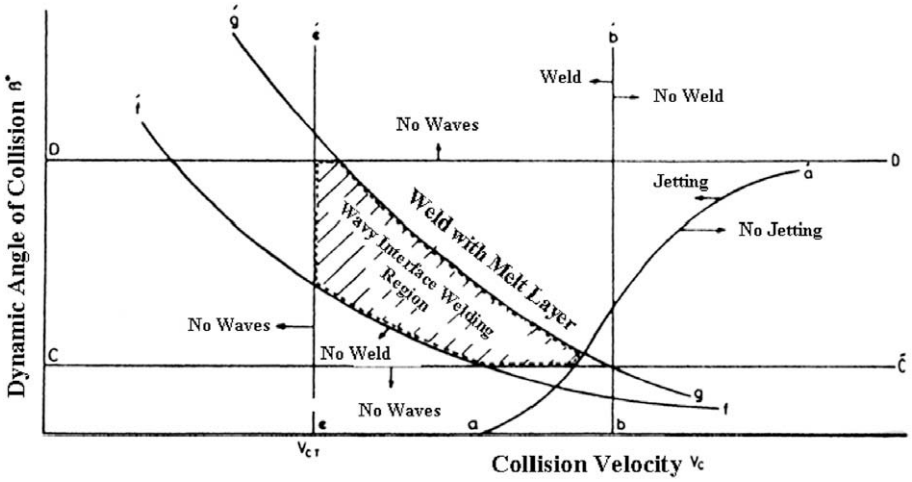

Fig. 4. Generic welding window.

Each welding couple has a specific Reynolds number for transition from straight into wavy interface, (see typical line "ee'" in Fig. 4). Reynolds number 8.7 is obtained for Ti/stainless steel couple. It should be noted that the fluid behavior is different from metal behavior during explosive welding. In explosive welding, for a very short time at the collision point, the material behaves like a fluid. In addition, the Eq. (1) was achieved for the collision angle of $\beta = 12^\circ$ and therefore, this relationship is not applicable for generic collision angle [1].

Other researchers proposed dynamic plasticity criterion for transition from straight to wavy interface. Dynamic plasticity plays a significant role for describing material behavior and wave properties at the collision point. Crossland and Williams [5], Wittman [8] and Al-Hassani and Akbari Mousavi [3] separately, proposed the following experimental Eqs. (2)–(4) for prediction of transition from straight to wavy interface.

$$\beta = \tan^{-1}(V_p/V_c) \tag{2}$$

where β is collision angle, V_c is collision velocity and V_p is flyer plate velocity. The flyer plate velocity is obtained from the following equation [8]

$$V_p = k_1(H_V/\rho)^{1/2} \tag{3}$$

where $k_1 = 1.14$ and H_v and ρ are the Vickers hardness and density of flyer plate, respectively. The proposed dynamic angle is [3]

$$\tan\beta = (3D\sigma_y/\rho V_c^2)^{1/2} \tag{4}$$

where D is damage constant that is taken 1.5 for titanium and σ_y and ρ are the yield stress and density of the flyer plate, respectively.

2.2. Weldability window

Wittman et al. [8,9] and Deribas et al. [10] developed an explosive welding window (Fig. 4), in which the collision angle β is plotted in the ordinates and the welding velocity, V_c is plotted in the abscissa. They studied jet formation, the critical impact pressure, the maximum impact velocity and wavy–smooth transition velocity. For example, if V_c reaches a supersonic value, there is no jetting. The same happens if the impact pressure is too low. The establishment of a weld ability window requires the relationship between the initial conditions (the initial angle α and the characteristics of the explosive) and the collision angle β.

In the present analysis, the same argument is used as that given by Birkhoff et al. [12], the direction of the velocity of the flyer plate bisects the angle SBC (see Fig. 3c). From geometry at the collision point (see Fig. 3c), the following equations can be obtained:

$$V_p = 2V_d \sin\left(\frac{\beta-\alpha}{2}\right) \tag{5}$$

$$V_c = V_p \frac{\cos\left(\frac{\beta-\alpha}{2}\right)}{\sin\beta} \tag{6}$$

where α is initial angle and β is collision angle.

One of the most important conditions for welding is the formation of a jet. Jetting has to occur at the collision point to achieve welding. In the theory if the velocity of collision point remains subsonic, jetting will occur. But in practice, however, a minimum angle is required to satisfy the pressure requirement, i.e. the pressure must be sufficient to exceed the dynamic elastic limit of metal to ensure deformation of metal surface into jet [1,5,10–12]. In [22], they calculated the critical angle for jetting for various metals and compositions as a function of detonation velocity for parallel set up geometry; $V_d = V_c = V_f$. Their results are shown in Fig. 5. The jetting occurs to the left of the lines in Fig. 5. In Fig. 4, line "aa" represents the critical angle β_c which is necessary for jetting. Abrahamson [13] proposed the following equation for jetting:

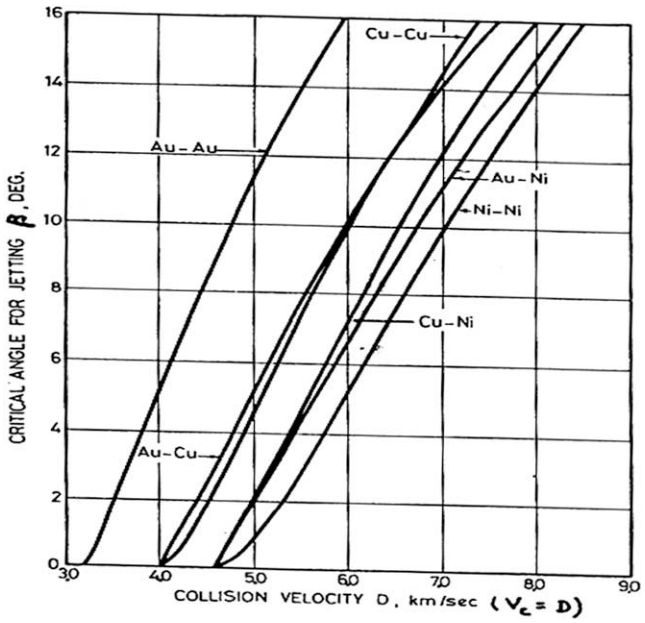

Fig. 5. The calculated values of critical β_c and V_d for parallel set up. Jetting occurs to the left of curves [22].

$$\beta = 10(V_c - 5.5) \tag{7}$$

where β is in radian.

Line "bb'" in Fig. 4, represents the upper limit of V_c estimated at 1.2–1.5 times the sound velocity [14]. It is however; experimentally evident that approaching the upper limit of V_c restricts the choice of other parameters within welding window. The Eq. (4) gives minimum collision velocity for bonding which is proposed by Simonov [24] as follows:

$$V_c = K(2H_v/\rho)^{1/2} \tag{8}$$

where K parameter is 2.5 for titanium and H_v is the Vickers hardness of material in MPa and ρ is the density of flyer plate in kg/m^3.

The lower and upper limits of the dynamic angle β were experimentally determined by Bahrani and crossland [25]. They suggested a lower limit of 2–3° and upper limit of 31° for collision angle for the parallel geometry. Maximum and minimum values of initial angles in an inclined system were suggested as 18° and 3°, respectively. In industrial applications where long plates are used, the inclination angle is set to zero and the parallel configuration is employed [1,5,10–12]. Stivers and Wittman [8,9] and Deribas et. al. [10] appears to agree that the lower limit for welding, line "ff" (see Fig. 4), is given in Eq. (9) as follows:

$$\sin\beta = k_2'\sqrt{\frac{H_v}{\rho V_c^2}} \tag{9}$$

where β is in radians, k_2 is a constant, H_v is the Vickers hardness, and ρ is the density. However, Deribas et al. [10] noted that Eq. (9) gives values different from experiment at large values of β, so they suggested the following equation for the lower boundary as

$$\beta = k_2\sqrt{\frac{H_v}{\rho V_c^2}} \tag{10}$$

The value of K_2 is 0.6 for high-quality pre-cleaning of surfaces, and 1.2 for imperfectly cleaned surfaces and 0.85 for general situations. The lower limit for bonding was also proposed by Blosinski [1] as follows:

$$V_c = \frac{V_p}{2\sin\left(\frac{\beta}{2}\right)} \tag{11}$$

where

$$V_p = 1.14\sqrt{\frac{H}{\rho}} \tag{12}$$

Deribas et al. [10], Crossland and Wittman [8,9] proposed two different equations for the upper limit for welding, line "gg'" (see Fig. 4). Wittman et al. [8,9] determines the value of V_p above which interfacial melting will occur, while the Deribas et. al. [10], accept that melting occurs and determine the condition that the time for solidification should be less than the time for tensile wave to reach the interface. Deribas et al. [10], Crossland and Wittman [8,9] relationships are given in Eqs. (13) and (14), respectively, as follows:

$$\sin(\beta/2) = k_3/(t^{0.25}\cdot V_c^{1.25}) \tag{13}$$

Table 1
Physical and mechanical properties of the titanium and AISI 304 stainless steel plates used in this study

Alloy	σ_y (MPa)	H_v (kg/m^3)	$C_{\text{shear sound velocity}}$(m/s)	ρ (kg/m^3)
Cp-titanium	280	180	6100	4500
AISI 304 stainless steel	450	210	5640	7900

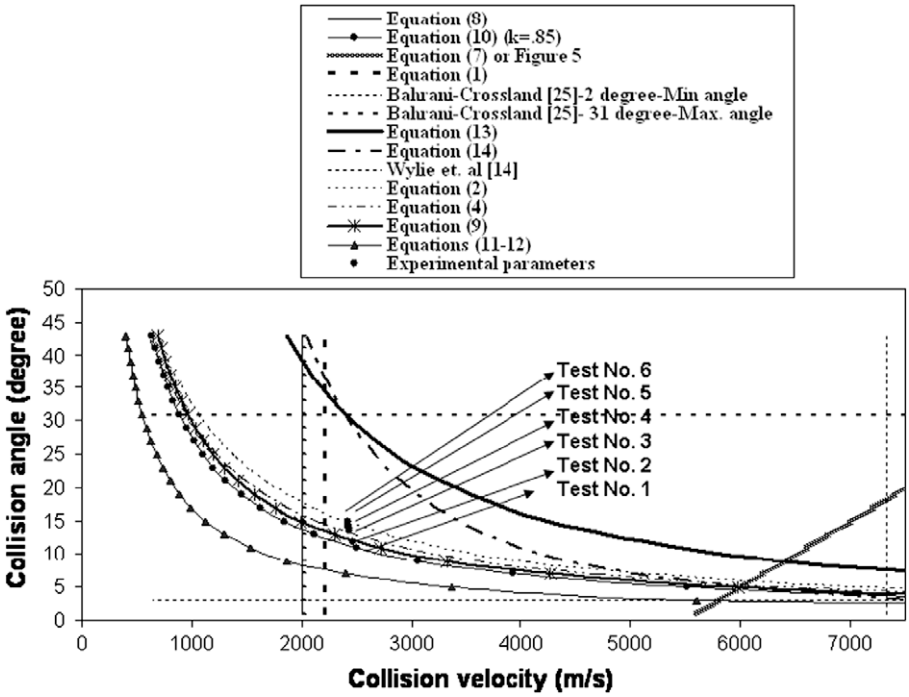

Fig. 6. Welding window of cp-Ti/AISI 304 stainless steel for explosive cladding with selected parameters. Eq. (8): Min (V_c) – for bonding by Simonov [24]. Eq. (7) or Fig. 5: boundary for jet formation by [13,22]. Bahrani and Crossland [25] Min β collision angle for bonding (2° angles) for parallel geometry). Bahrani and Crossland [25] Max β collision angle for bonding (31° angles) for parallel geometry). Eq. (13): Deribas upper limit for bonding [10]. Eq. (14): Wittman upper limit for bonding [8,9]. Eq. (10): Deribas lower limit for bonding [10]. Eq. (9): Wittman, Stiver and Deribas lower limit for bonding [8–10]. Eq. (11), (12): Blosinski lower limit for bonding [1]. Wylie et. al [14]: Max V_c collision velocity, 1.2–1.5 times the sound velocity. Eq. (4): Al-Hassani criteria for transition from straight to wavy interface [3]. Eq. (1): hydrodynamic criteria for transition from straight to wavy interface [21–23]. Eq. (2): Crossland criteria for transition from straight to wavy interface [5].

$$V_p = k_4/t^{0.25} \cdot V_c \tag{14}$$

where $k_3 = C_f/2$, $C_f = (K/\rho)^{1/2}$, $K = E/3(1-2v)$, t is the thickness of flyer plate and $k_4 = 2.86 \times 10^6$ for titanium as flyer plate in this study, K is the bulk modulus and C_f is shear wave velocity.

The physical and mechanical properties of cp-titanium and stainless steel used in this study are given in Table 1. Welding window of cp-titanium to 304 stainless steel is developed based on Eqs. (1)–(14) and plotted in Fig. 6. Fig. 6 also shows the operational parameters used in our experiments.

3. Experiments

3.1. Experimental procedures

3.1.1. Materials and explosive joining

The commercial pure titanium and AISI 304L stainless steel annealed plates are used in the present work. The dimensions of titanium and stainless steel plates used in this study were $200 \times 250 \times 4$ mm and $200 \times 250 \times 8$ mm, respectively. The surface of the base and flyer plates were used as received. Their chemical compositions are given in Table 2.

Due to mechanical and corrosion properties of titanium and stainless steel, they were chosen as overlay plate and base plate, respectively [5,10]. In this investigation, a low detonation velocity explosive of 2400 m/s and density of 850 kg/m^3 was used. The parallel set-up geometry is employed in all experiments and all explosions were carried out on a sand anvil. In order to investigate the effects of explosive loading on bonding interface, the experiments were designed and their parameters were chosen by numerical simulations using ABAQUS code. The Williamsburg-type equation of state was employed to model low detonation velocity ANFO explosive [3,4,16]. The explosive welding parameters used in this study are listed in Table 3. The numerical values were obtained from the simulation results.

Table 3
Selected parameters for explosive cladding

Test No.	Explosive loading (R)	Stand-off distance (mm)	Collision velocity (m/s)	Impact velocity (m/s)	Collision angle (β)	Collision energy (J/cm^2)
1	0.5	2	2460	523	12.0	246.2
2	1.0	2	2426	591	13.7	314.4
3	1.2	2	2421	605	14.0	329.4
4	1.5	2	2387	615	14.3	340.4
5	2.0	2	2383	627	14.5	353.8
6	2.5	2	2382	641	14.9	369.8

3.1.2. Microstructure work

To reveal the microstructure aspects of interface, the specimens were cut parallel to detonation direction. The cross-section of spec-

Table 2
Chemical compositions of the materials used in this study (weight percent %)

Alloy	C	Fe	Ti	Mn	P	Si	S	Cr	Ni	Mo	Cu	Al
cp-Ti	0.20	0.32	Bal	–	–	–	–	–	–	–	–	0.20
304 stainless steel	0.01	Bal	–	1.15	0.045	0.23	0.09	21.20	8.42	0.03	.09	–

imens were ground with emery papers up to No. 1500 and polished with diamond paste. Then Ti-sides were etched in an aqueous solution of 3 ml HF, 5 ml HNO3 and 92 ml H_2O and stainless steel-sides were etched separately in a solution containing a mixture of 1:3 HNO_3 and HCl. The observation of the structural changes due to explosive cladding process were examined by optical microscope (Correct, SDME), and scanning electron microscopy (SEM, Cam Scan 2300 MV), equipped with energy-dispersive X-ray spectrometry (EDS). A set of bonded assemblies were fractured under lug-shear test and reaction products on Ti-sides were detected by X-ray diffraction (XRD, Philips X́ pert), using a Cu target at an operating voltage of 30 KV and current of 20 mA. Scanning span was 20–95° with step size of 0.02° and speed of 0.02°/s.

3.2. Results and discussion

One of the purposes of this study is to develop the welding window of cp-titanium to 304 stainless steel using the expressions proposed by various authors (see Eqs. (1)–(14)). The next step is to find the locations of the operational parameters of the experiments carried in this study (see Table 3). The collision velocity-collision angle was determined for each test by the simulations. The results are depicted in Fig. 6. It is shown in Fig. 6 that all the experiments are within the welding window. The experiment carried out with $R = 0.5$ is located on the lower boundary of welding proposed by Wittman [8,9] and Deribas [10] (Eq. (10)). Therefore, the welding window predicts that the welding has to occur. However, the experiments show no welding for $R = 0.5$. The experiments performed with R = 1 is positions slightly above the lower boundary of welding proposed by Wittman [8,9] and Deribas [10] (Eq. (10)). The operational parameter of this test is located on the Wittman [8,9] curve (Eq. (9)). The welding window predicts that the straight interface has to be obtained for $R = 1$. This result is confirmed by optical micrographs (see Fig. 7a). The welding window predicts the transition from straight to wavy interface for the test performed with $R = 1.2$, because, it is located very close to the Al-hassani transition curve (see Fig. 6) Eq. (4). The metallographic study confirms the transition from straight to wavy interface for $R = 1.2$ experiment (see Fig. 7b). The welding window predicts the transition from straight to wavy interface for the tests performed with $R = 1.5$, $R = 2$ and $R = 2.5$. Because, they are located slightly above the Al-hassani transition curve (see Fig. 6) Eq. (4) and slightly below the Crossland transition from smooth to wavy interface curve (see Fig. 6) Eq. (2). However, the optical microscopy of the welding interface for the test performed with $R = 1.5$ shows the wavy interface (see Fig. 7c). The wavy with vortices interfaces are obtained for the tests with $R = 2$ and $R = 3$ (see Fig. 7d and e).

In additions, all the tests are to the right of the transition from smooth to wavy interface line based on the hydrodynamic analysis (Eq. (1)). Therefore, according to this theory, the welding window

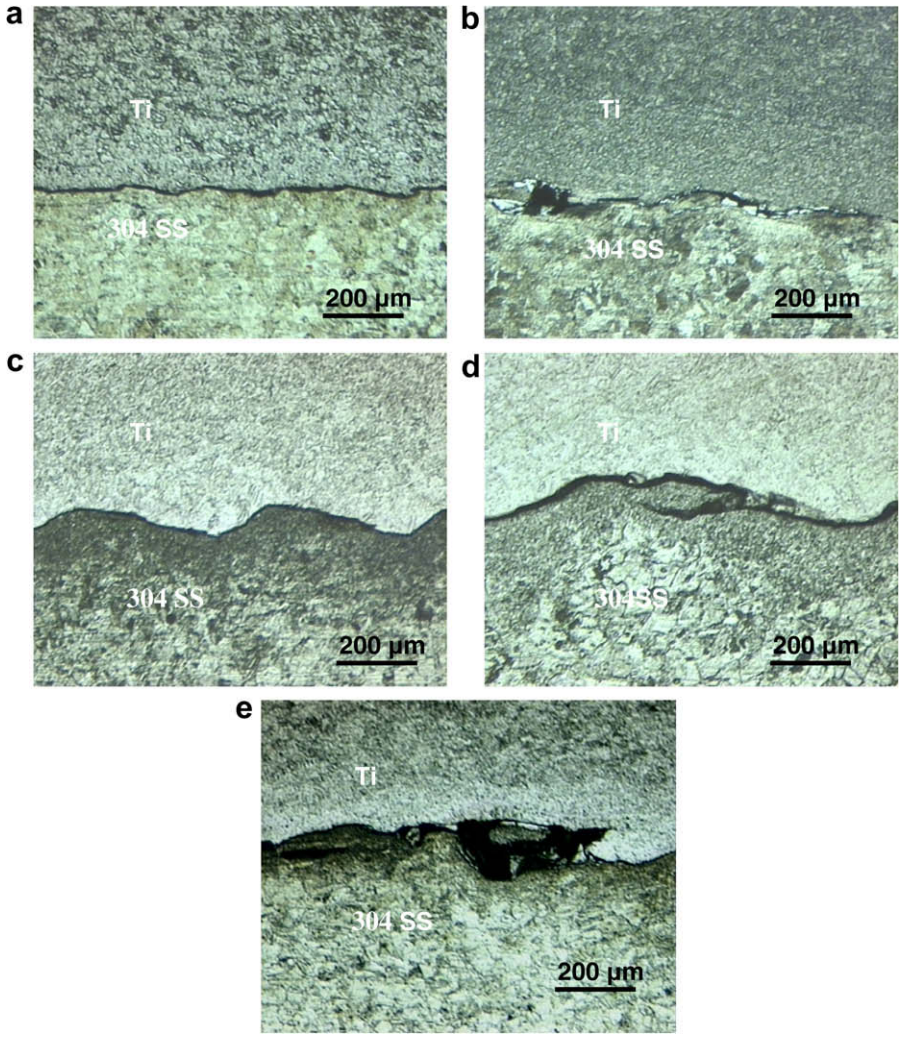

Fig. 7. Optical micrographs from the interface of cp-titanium/AISI 304 stainless steel for different explosive loads: (a) $R = 1$, (b) $R = 1.2$, (c) $R = 1.5$, (d) $R = 2.0$, (e) $R = 2.5$.

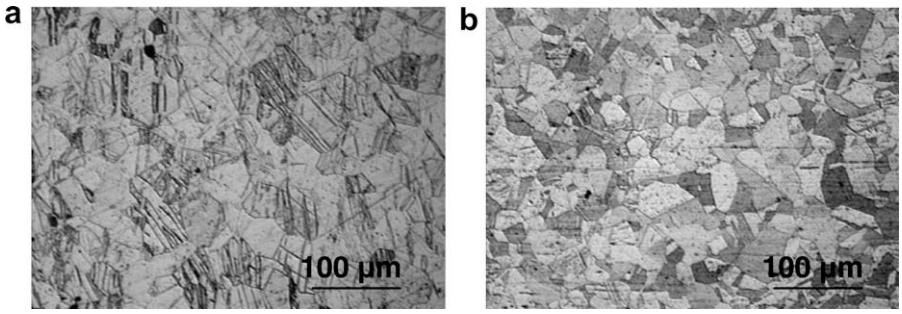

Fig. 8. The microstructure of: (a) Cp-titanium and (b) AISI 304 stainless steel, from optical microscope.

predicts the wavy interfaces for all the tests carried out in this study. However, the metallographic studies do not confirm this finding (see Fig. 7a–e).

3.2.1. Metallographic studies

The optical figures of titanium and stainless steel are shown in Fig. 8. Fig. 8a show the cp-Ti microstructure which is mainly composed of equiaxed α-Ti grains with mechanical twins. Fig. 8b shows fully austenite equiaxed grains for AISI 304 stainless steel.

Most of the experiments performed in this study were successful. Good bonding was achieved in all experiments except test No. 1 with $R = 0.5$ (see Table 3). The explosive welding parameters for the experiments carried out in this study are suited in the proper locations of the welding window (see Fig. 6). Since the tests were performed with low explosive loads with low welding energy, the surface roughness plays an important role in welding. Since the jet has to form in order to bonding occur, thus the amount of energy must be enough for jetting to occur. In test No. 1, no welding occurred, though theoretically jetting was produced, however, the impact angle was not sufficient to produce the necessary impact pressure for bonding. In addition, jetting did not produce from both surface plates, i.e. higher energy is required to form the jet for the rough surface. Effects of surface roughness cannot be included properly in the simulations. Therefore, it is concluded that the predictions related to types of the interfaces obtained by welding window might be deviated from that achieved by experiments, since the surface roughness parameter is not considered properly in developing the welding window. Fig. 7 illustrates the optical micrographs of explosive weld interfaces for different explosive loads.

The high pressure shock waves that develop during the collision of plates cause extensive plastic deformation at the contact regions. Grains near the interface were generally elongated parallel to the impact direction. Etching of the interface and its vicinity denote a complex pattern of plastic flow and anisotropic stress distributions, as shown in Fig. 7a–e. Optical micrographs in Fig. 7 show the effects of interface morphology with explosive loads. The least waviness is seen in Fig. 7a ($R = 1.0$). Fig. 7 shows that the waviness increases with explosive loading. In some cases sever deformation of the waves may lead to the separation and drifting of wave crests, (see Fig. 7d–e). Because of difference between density of titanium and stainless steel, the shape of the waves formed in the interface is asymmetric. At excessive explosive loads, vortices are formed, (see Fig. 7d and e). The vortex of waves can exhibit localized melting. It is related to adiabatic heating of trapped jet inside vortices at the front slope of waves as a result of density difference or the adiabatic heating of gases compressed between the plates. When the melting is produced at the vortices, (see Fig. 9), the deformation of solid material is transformed into circular movement and vigorously stirring of molten materials which in turns leads to intermingling of both Ti and stainless steel. Generally, the basic metal of vortex (stainless steel) is deformed into thin lamella, which is in the form of spiral. The molten zone is surrounded by relatively cold metal and subjected to a very high cooling rate. The cooling rate was estimated to be of the order of 10^5–10^7 K/s [6]. Typical defects in the vortices due to solidification as can be seen in Fig. 9 are shrinkage, cracks and gas porosity.

Table 3 shows that the impact energy and velocity increase with explosive loading at the collision point. The explosive loading increases the collision pressure and plastic deformation at the interface. The reason is attributed to the increase of tangential component of impact velocity and the shearing stresses produced between the impacting metals. Moreover, the wavelength and amplitude are increased with explosive loading. The average dimensions of waves formed in the interface during welding for different impact velocity are shown in Fig. 10. Increase in wavelength and amplitude with explosive loading was also reported by previous researchers [2,15–20].

Fig. 7 shows the refinements of grain size at the interface. The grains are coarsened away from the interface. The reason is attrib-

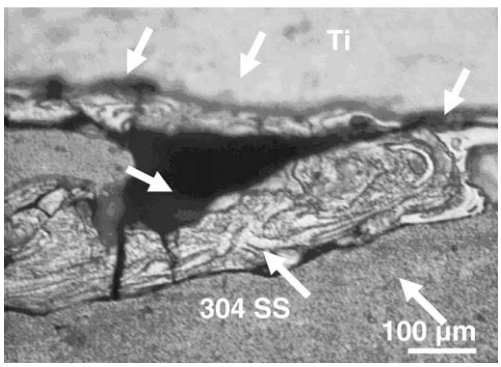

Fig. 9. Optical micrograph from the interface at higher magnification for $R = 2.0$.

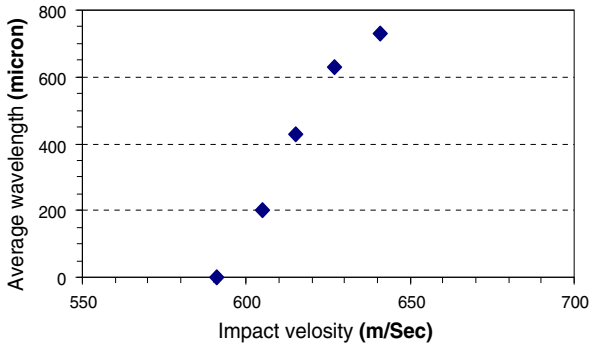

Fig. 10. Variation of average wavelength with impact velocity at the interface.

uted to the induced plastic deformation in the interface during explosion. In this work, the morphologies of the interface showed that explosive loads are not only sufficient to have transition from straight to wavy interface but also to obtain wavy interface with vortices.

3.2.2. SEM studies

Fig. 11 illustrates the SEM-BSE micrographs of explosive welded interfaces for different explosive loads. SEM micrographs show that the interface was outlined by characteristic sharp transition between two materials, but local melted zones were also encountered in the front slope of waves in the interface which is in agreement with optical micrographs. If kinetic energy is further increased, the melted zones grow and coalesce to form a semi continuous interlayer, Fig. 11d–e.

Review of the metallurgy of explosive welds between metals with very different densities in the literature shows a greater possibility for the formation of what appears to be a thin intermetallic cast interlayer in the interface [2,17–20]. SEM micrographs confirm this matter (see Fig. 11a–e). Two types of interfaces generally exist in the explosively welded composites; these are metal-metal and metal-solidified melt, (see Fig. 11a–e). Band formation is observed between the local melted zone and flyer plate, (see Fig. 11a–e). This can be attributed to the thermal conductivity of titanium which is lower than that of stainless steel. This means that during the solidification of the melted zone, heat was sluggishly conducted from melted zone to titanium and cause to form such a region. Due to the brittle nature of intermetallic phases formed between titanium and stainless steel, the cracking is occurred in the interface.

3.2.3. XRD studies

X-ray diffraction studies were preformed on the cp-Ti and 304 stainless steel. The result confirms that these materials exhibit hexagonal close packed and f.c.c systems, respectively, at room temperature. XRD were carried out on the cp-Ti side of the fractured samples to investigate the different phases formed near the interface due to diffusion at various collision temperatures for various explosive loads. The results of X-ray diffraction on the Ti side of assemblies are shown in Fig. 12.

No intermetallic phases were detected for specimen welded by low explosive load, Fig. 12a. Moreover, only titanium oxides, such as Ti_2O_3 and TiO, were detected on the fractured surface. At low explosive load and low impact energy, the removal of surface oxides due to the low energy of jetting does not perform completely and therefore, titanium surface oxides, Ti_2O_3 and TiO, are remained in interface of composite which can be detected. In addition, because of low impact energy during welding, a little amount of intermetallic phases may be formed in the interface and they may be so small that cannot be detected by XRD. This result is in agreement with SEM micrograph (see Fig. 11a). By increasing the explosive load, different intermetallic phases are detected by XRD, (Fig. 12b–d). These intermetallic phases are Fe_2Ti_4O and Fe_2Ti for specimen welded with $R = 1.2$, Fig. 12b, and Fe_2Ti_4O, Fe_2Ti and Cr_2Ti for specimens welded with $R = 2$ and 2.5, (Fig. 12c–d). In

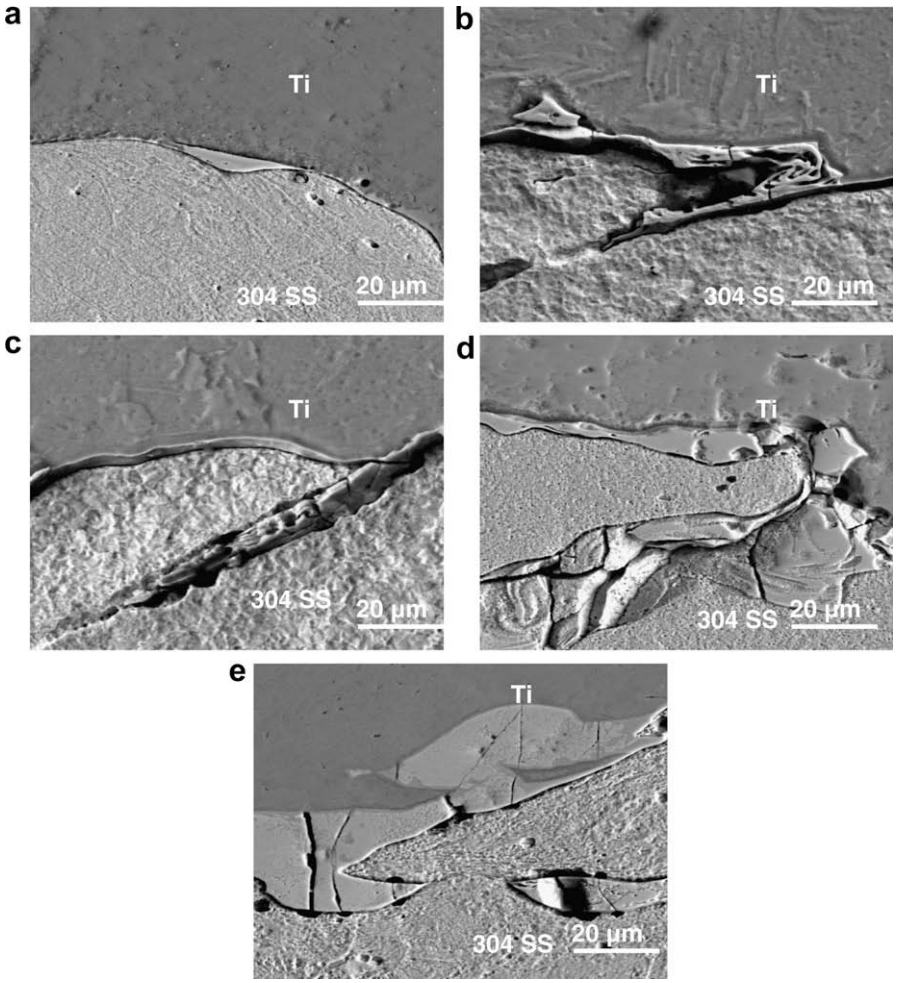

Fig. 11. SEM-BSE micrographs from the interface of cp-titanium/AISI 304 stainless steel for different explosive loads: (a) $R = 1$, (b) $R = 1.2$, (c) $R = 1.5$, (d) $R = 2.0$, (e) $R = 2.5$.

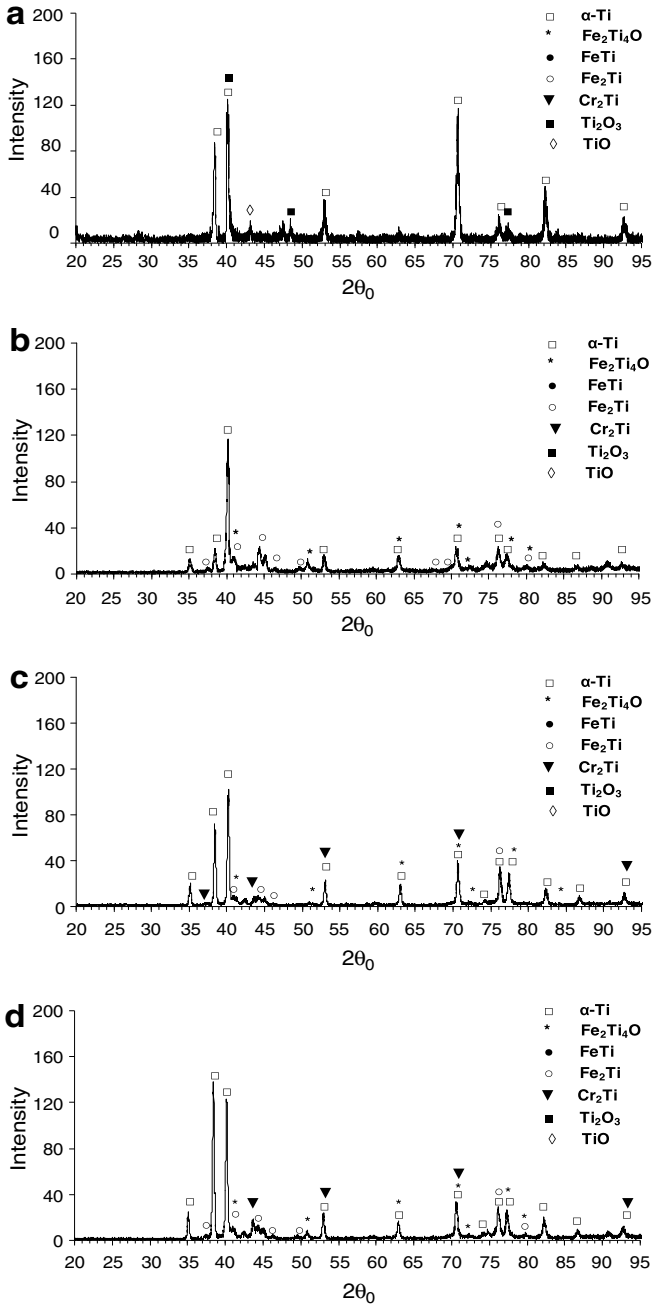

Fig. 12. X- ray diffraction analyses for the fractured surfaces of the titanium sides, for different explosive loads: (a) $R = 1$, (b) $R = 1.2$, (c) $R = 2.0$, (d) $R = 2.5$.

these cases, higher impact energy causes formation of more amount of melting sites in the interface due to dissipation of impact energy at the collision point. The melting sites are subjected to high cooling rate due to cold surroundings during solidification. Penetration of constituent elements into the molten zones is increased with the explosive load. The limited solubility of Fe, Cr and Ti in the solid state causes to from different phases in the interface. Therefore, Fe_2Ti_4O and Fe_2Ti are formed for specimen welded with $R = 1.2$ and by increasing the explosive loads, Cr_2Ti is observed as a result of more penetration of Cr into the molten zones which is enough for phase formation in the solid state. Formation of Fe_2Ti_4O can be related to presence of hot compressed air due to adiabatic heating at the collision point which causes high driving force for the formation of this oxide phase at the molten sites in the interface during the explosive welding process.

4. Conclusions

The objective of this study was to establish the conditions for straight, wavy weld formation in the explosive welding of cp-Titanium and AISI 304 stainless steel. The weldability domain was defined and was successfully used to predict the proper welding parameters for welding. It is a useful object in order to tailor welding conditions and is applicable to the experimental results containing both wavy and smooth domains. Explosive welding of cp-Ti and AISI 304 stainless steel under different explosive load were carried and micro-structural features of interfaces were investigated. The following conclusions can be drawn:

- At low explosive load, the flat interface is produced. The wavy interface is produced at higher explosive loads.
- Wavelength and amplitude of waves are increased with explosive loads.
- Grains near the interface were elongated along the explosive direction due to high localized plastic deformation produced during collision of the plates.
- Grains near the interface are more refined with the explosive loads.
- SEM studies show the formation of melted sites in the interface especially at the crest and front slope of waves which grow with explosive load.
- A number of brittle intermetallic phases such as Fe_2Ti, Fe_2Ti_4O and Cr_2Ti are identified in the interface at high explosive loads.

References

[1] Blazynsky TZ. Explosive forming welding and compaction 1983. Applied Science Publishers LTD.
[2] Rughue N. Characterization of explosive weld interface. In: Proc intern symp res stud mat sci eng, Chennai, India; December 2004.
[3] Akbari Mousavi SAA, Al-Hassani STS. Numerical and experimental studies of mechanism of wavy interface formations in explosive/impact welding. J Mech Phys Sol 2005;12:251–79.
[4] Akbari Mousavi SAA, Al-Hassani STS, Burley SJ. Simulation of explosive welding using the Williamsburg equation of state to model low detonation velocity explosives. Int J Imp Eng 2005;31:719–34.
[5] Crossland B, Williams JD. Explosive welding. Met Rev 1970;15:79–100.
[6] Hammerschmidt M, Kreye H. Met Char Exp Weld Zone. 1984;37(7): 12–21.
[7] Loyer A, Talerman M, Hay DR. Explosive welding: the weldability window for dissimilar metals and alloys. In: Third int symp use exp ene manuf metallic mat new prop; 1976. p. 43.
[8] Wittman RH. Use of explosive energy in manufacturing metallic materials of new properties. In: Second int symp, Marianski, Lazne, Czechoslovakia; 1973.
[9] SW, Wittman RH. Computer selection of the optimum explosive loading and welding geometry. In: Proc fifth int conf high ener rate fab, vol. 4(2); 1975. p. 1–16..
[10] AA, Simonov VA, Zakcharenko ID. Investigations on explosive welding parameters for arbitrary combinations of metals and alloys. In: Proc sixth int conf high ener rate fab, vol. 4(1); 1975. p. 1024..
[11] Bahrani AS, Crossland B. Explosive welding and cladding: an introductory survey and preliminary results. Proc Inst Mech Eng 1964;79:264.
[12] Birkhoff G, MacDougall DP, Pugh EM, Taylor G. Explosive with lined cavities. J Appl Phys 1948;19:563–82.
[13] Abrahamson GR. Permanent periodic surface deformations due to a traveling jet. J Appl Mech 1961;83:519–28.
[14] Wylie HK, Williams PEG, Crossland B. Further experimental investigation of explosive welding parameters. In: Proc second int conf cen high ener fab, vol. 1(3); 1971. p. 1–43.
[15] Pocalyko A. Fabrication of explosive-welded titanium-clad composites. Weld J 1987:24–30.
[16] Akbari Mousavi SAA, Al-Hassani STS, Byers Brown W, Burley SJ. Simulation of explosive welding with ANFO mixtures. J Prop Expl Pyrot 2004;29(3):188–96.
[17] Kahraman N, Guence B, Findik F. Joining of titanium/stainless steel by explosive welding and effect on interface. J Mat Proc Technol 2005;171: 241–9.
[18] Kahraman N, Guence B. Microstructural process mechanical properties of Cu–Ti plates bonded through explosive welding. J Mat Proc Technol 2005; 169(1):67–71.
[19] Acarer M, Guenç B. Investigation of explosive welding parameters and their effects on microhardness and shear strength. Mat Des 2003;24:659–64.

[20] Banker JG, Winsky JP. Titanium/steel explosion bonded clad for autoclaves and vessels. Clad Metal Prod Inc; 2000.
[21] Holtzman AH, Cowan GR. Bonding of metals with explosive. Weld Res Counc Bull 1965;104:1–21.
[22] Holtzman AH, Cowan GR. Flow configuration in colliding plates: explosive bonding, J. Appl Phys 1963;34:4. Part 1: 928-939.
[23] Cowan GR, Bergman OR, Holtzman AH. Mechanics of bond wave formation in explosive cladding of metals. Met Trans 1971;2:3145.
[24] Simonov VA. Binding criteria for metals with explosive welding. Comb Expl Shock Wav 1991;27(1):121–3.
[25] Bahrani AS, Crossland B. Some observations on explosive cladding. In: Weld ann conf AD, ASTME; 1966. p. 66–112.